Comparative Study of an Open Waveguide. Application to Deconvolution of a Magnetic Probe in Near-Field Zone

A. Saghir[1], C. Avram[2] J. Tao[*,3]
[1, 2,3] Laplace ,site ENSEEIHT
*ENSEEIHT, 2 rue Camichel, 31071 Toulouse, tao@laplace.univ-tlse.fr

Abstract: We present here our work on deconvolution of a magnetic probe to measure electromagnetic emissions in near-field zone. To achieve this work, we have chosen a rectangular waveguide (WR90) as a radiating structure. Theoretical near-field is simulated using a FEM software (COMSOL) and also obtained by using a program based on transverse operator method (TOM) ,that lead to a very good field reconstruction after deconvolution due to its precision.

Keywords: Open waveguide, deconvolution

1. Introduction

The presence of electric or magnetic probes used in near-field measurements surely perturbs the measured parameters .In the case of the loop magnetic probe used here, the induced electromotive force is proportional to the number of field lines crossing through it .Probes' influence has an effect of integration which is manifested through reducing the spatial resolution of field's real image.

In order to identify then correct the effect of these perturbations .We have convolved the field's original distribution $f(x,y)$ with response function $r_p(x,y)$, characteristic function of the probe

$$d(x,y) = r_p(x,y) * f(x,y) + n(x,y) \quad \ldots \quad (1)$$

For a known source $f(x,y)$ near-field measurement $d(x,y)$ in optimal conditions minimizes measurement's noise $n(x,y)$. We obtain probe's transfer function $r_p(x,y)$ by deconvolution process explained below.

2. DECONVOLUTION THEORY

First , suppose that the probe is placed in a fixed position with respect to the measurement antenna .Output voltage of the probe depends on field's value at the probe's position in the presence of the probe itself . In time domain, we define the following: $r_p(t)$ probe's transfer function $b_1(t)$ field value emitted by the antenna at the position of the probe, and $b_p(t)$ probe's output voltage. Neglecting noise and considering that the probe making scan at discrete points (output function does not depend on probe's scanning surface) these parameters will be related by convolution's law

$$b_p(t) = r_p(t) * b_1(t) \quad \ldots \quad (2)$$

Replacing $b_1(t)$ by Dirac-delta function (spectrum $B_1(\omega)$ will be constant not depending on the pulsation while $r_p(t)$ is measured directly).

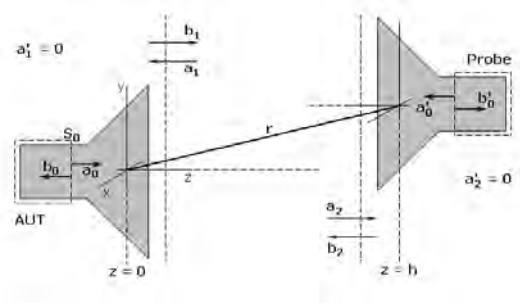

Fig.1 Schematic diagram of a measurement system

In measurement phase, problem complexity rises slightly since we have to dispose (carry out) many measurements to describe Dirac frequency response. Using network analyzer, we have to measure probe's output signal spectrum in a wide frequency band at a constant input power which is not easy to do because the used structure is a rectangular waveguide having a limited frequency band. In this case, we have to use a structure transporting a TEM mode and the probe's response function will be simply the inverse Fourier transform of measured spectrum

$$r_p(t) = \mathcal{F}^{-1}\{B_p(\omega)\}, \quad for\ B_1 = ct., \omega = [0,\infty] \quad ..(3)$$

The adopted approach in this article is to define and solve the deconvolution problem in spatial domain or in other words our aim is to

increase the spatial resolution of near-field measurements.

The formulation of near-field measurements correction presented here is an adaptation of near-field measurements theory elaborated by Kerns [1]

Kerns hypothesis considers that multiple interaction between probe measured structure (circuit) are negligible, or we can say that the radiated field by induced sources at the level of the probe is too small for its reflection at measured structure's (circuit) level to be recaptured by the probe.

Probe's output signal under incidence of circuit's radiated field in measurement plane ($z=h$) is given by the following plane wave decomposition

$$\mathsf{b}_p(\mathsf{r}_0) = a_0 e^{-j\gamma z_0} \int_{-\infty}^{+\infty}\int_{-\infty}^{+\infty} \mathsf{R}_p(k_x,k_y)\cdot \mathsf{B}_1(k_x,k_y) \cdot e^{-j(k_x x_0 + k_y y_0)} dk_x dk_y \quad (4)$$

3. OPEN GUIDE MODEL in COMSOL and TOM.

As mentioned above our model is a rectangular waveguide radiating into free space as in the figure (2). There are many methods to model this guide from which we used two: COMSOL (FEM) and transverse operator method (TOM)

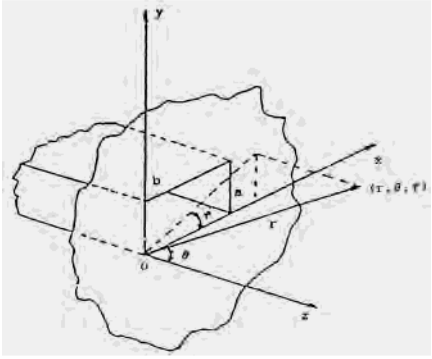

Fig.2 – Radiating open waveguide

Finite element method is an efficient technique to analyze not only simple structures but also complex ones giving precise and fast solutions to different systems of differential equations.

FEM initially used by P. Silvester[2] for electromagnetic field problems and produced numerical algorithms in many fields of applications, dividing the problem into small divisions which may be composed of triangles, tetrahedrals, or their combination that may adapt simply to the geometry .

FEM mesh elements may be simply modified (fine or coarse) in different regions of the structure, giving rise to precise solutions as compared to other analytical methods.

COMSOL multiphysics facilitates all steps in modelling process as defining the geometry, specifying the physics, mesh generation, solving and then post-processing the results as we have done in our rectangular waveguide (WR90) which is designed to maintain energy losses due to reflections at a minimum in our band of operation between 8.2 GHz -12 GHz.

To study the characteristics of this waveguide, consider a wave travelling through the rectangular waveguide into free space. The S-parameters are calculated as functions of the frequency leading to the deduction of admittance.

The input port is excited by a TE_{10} wave, which is the only propagating mode, with an input power 1W in the second phase of simulation process while in the first one ,we have solved only for effective mode index.

The model treats the metallic walls of the waveguide as perfect electric conductors satisfying the boundary condition

$$n \times \mathrm{E} = 0 \ldots \quad (5)$$

The propagating mode is obtained from the solution of an eigenmode problem at the first port at which the solved eigenmode equation is

$$\nabla \times (n^{-2} \nabla \times \mathrm{H}_n) + (n^{-2}\beta^2 - k_0^2)\mathrm{H}_n = 0 \quad \ldots.(6)$$

Here H_n is the component of the magnetic field perpendicular to the boundary, n the refractive index, β the propagation constant in the direction perpendicular to the boundary, and k_0 the free space wave number. The eigenvalues are $\lambda = -j\beta$.

The effective mode index is $\beta/k_0 = 0.755$ at 10GHz frequency (only real one is taken into account), corresponding to the TE_{10} mode.

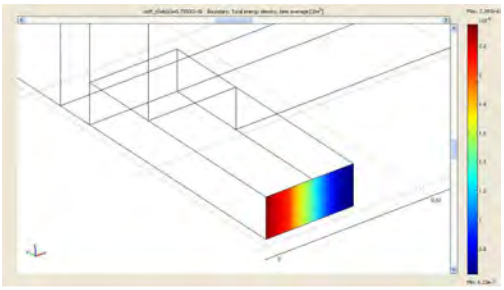

Figure 3: Input port total energy density lead to the generation of first eigenmode with effective mode index =0.755

Also we'll explain TOM theory briefly

In order to have an equation for the electromagnetic field at the flange plane,we can rewrite Maxwell's equation, declaring that z is the direction of propagation , in the form

$$\hat{L}\phi(x,y,z) = j\eta\frac{\partial}{\partial z}\phi(x,y,z)\ldots\ldots \quad (7)$$

$$\eta = \begin{bmatrix} 0 & 0 & 0 & -j \\ 0 & 0 & j & 0 \\ 0 & -j & 0 & 0 \\ j & 0 & 0 & 0 \end{bmatrix}, \quad \phi^t = [E_t \quad j120\pi H_t]$$

ϕ' is the transversal field vector

$\hat{L}$ is the deduced transverse operator of Maxwell's equation [3].

A particular solution of this equation in the presence of propagating waves in free space is obtained in the form of these two equations [3]

$$\frac{k_0}{2\pi}h_0^{(2)}\left(k_0\sqrt{x^2+y^2}\right) * \hat{L}_0 E_{t0} = 120\pi\eta_0 H_{t0} \ldots (8)$$

$$\phi(x,y,z) = \frac{1}{2\pi^2}\iint \tilde{\phi}_0(p,q)\, e^{j[px+qy-\omega(z-z_0)]}dpdq \ldots (9)$$

Where ϕ_0 corresponds to fields at the flange plane z=z$_0$ and $\hat{\phi}_0$ is its two dimensional Fourier transform.

In the case where the structure is fed by a TE$_{10}$ mode, the fields at the flange level (discontinuity level) are a linear combination of TE$_{10}$ (incident and reflected) as high order modes generated by the discontinuity or existing at its level.

Equation 8 permits to obtain the generalized S matrix of the structure; later ϕ_0 is deduced allowing to calculate the radiated fields into the free space by using eq. 9.

Where $R_p(k_t)$ is the Fourier transform of the probe's characteristic function and $B_1(k_t)$ is total plane waves which contributes to antenna's radiation spectrum .

Calculation formula of emission spectrum of an antenna with probe correction is given by

$$\mathrm{B}_1(k_x,k_y) = \frac{e^{j\gamma z_0}}{4\pi^2 a_0}\mathrm{R}_\mathrm{p}^{-1}(k_x,k_y) \cdot\int_{-\infty}^{+\infty}\int_{-\infty}^{+\infty}\mathrm{b}_\mathrm{p}(\mathrm{r}_0)\cdot e^{j(k_x x_0+k_y y_0)}dx_0dy_0 \quad (10)$$

The double integral in the right side of eq (10) is simply the Fourier transform of field data obtained from near-field measurements by planar scanning in the surface of measurements.

The radiated field to free space is found again by the product of probe's characteristic of inverse reception and Fourier transform of probe's output obtained by measurements.

Another hypothesis used in this approach of deconvolution is that the probe is only sensible to certain field components. In our case, a magnetic loop probe is used, sensitive essentially to one of magnetic field transverse components. In fact, this hypothesis is valid because we have measured an attenuation greater than 20dB in cross polarization with respect to nominal polarization of the loop.

Where $b_p(r_0)$ corresponds to a modelled radiating structure, the same approach will be employed in order to determine the characteristic function of the probe, for this reason eq (10) may be rewritten in the following form

$$\mathrm{R}_\mathrm{p}(k_x,k_y) = \frac{e^{j\gamma z_0}}{4\pi^2 a_0}\mathrm{B}_1^{-1}(k_x,k_y) \cdot\int_{-\infty}^{+\infty}\int_{-\infty}^{+\infty}\mathrm{b}_\mathrm{p}(\mathrm{r}_0)\cdot e^{j(k_x x_0+k_y y_0)}dx_0dy_0 \quad (11)$$

4. Results and Discussion:

Magnetic field x-component is calculated using eq9 on a plane parallel to that of the flange at a height of 10mm. A simulation is made also using COMSOL multiphysics[4]. The comparison is shown in figure 4 for normalized H_x magnitude. We notice the same variation with results obtained by TOM are more concentrated and give more precision in spatial resolution.

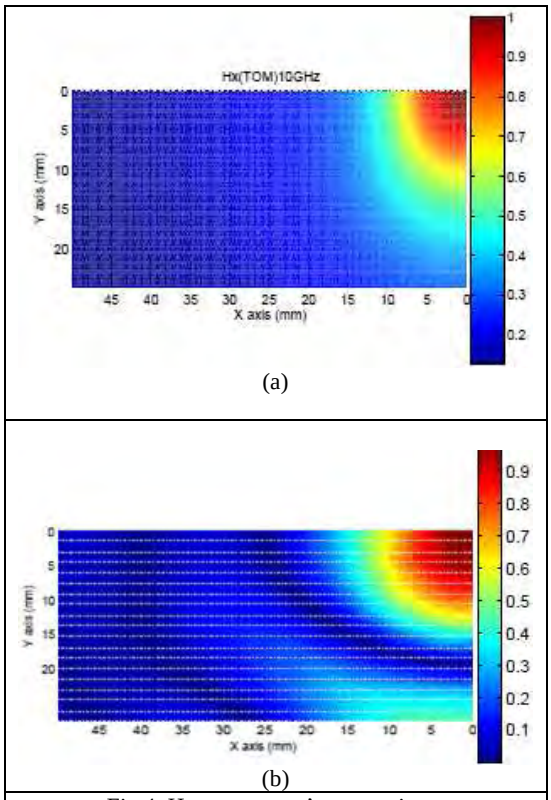

Fig 4: Hx component's comparison.
H_x component at 10mm height obtained by TOM (a) and COMSOL (b) respectively

Reflection coefficient is calculated using COMSOL and TOM showing good agreement between them.

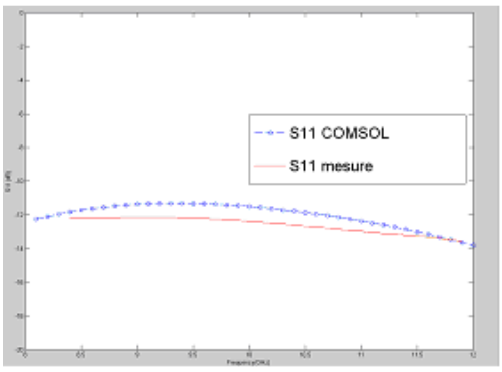

Fig.5: S11(dB) as a function of frequency.

Moreover, figure (6) shows the equivalent admittance of the structure, given by

$$Y=(1-S)/(1+S)$$

We notice that COMSOL admittance is slightly far from that of TOM except near to the frequency 10GHz.

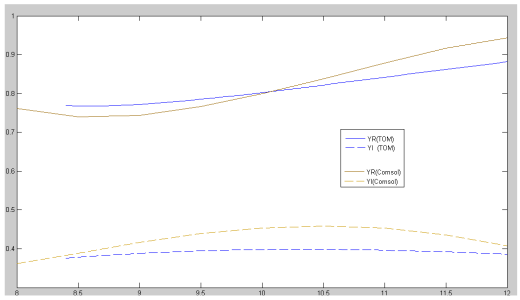

Fig.6: Admittance as a function of frequency.

This may be explained by the finite size of entire structure while in TOM we consider an infinite half space.
Other tests will be presented during the conference.

4.1. Probe Deconvolution in Transverse Magnetic Field

Measurement is done to obtain transverse magnetic field component H_x on a surface $60*60mm^2$ at a height of 10mm with a step 1mm.
Measurements made in a convenient environment employing absorbers to avoid reflections caused by metallic parts of workbench at the flange level.

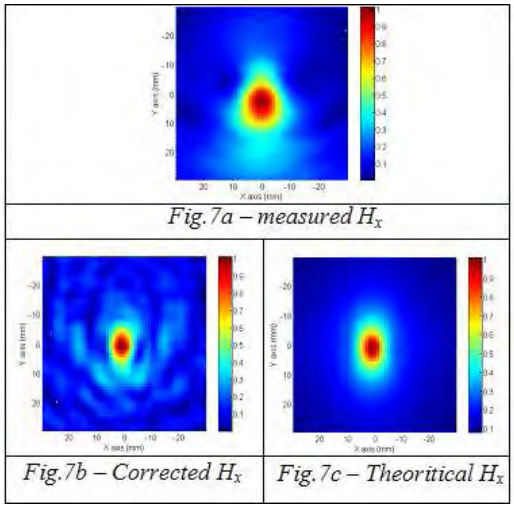

Fig.7: Comparison between measured (a), theoretical (c) and corrected (b) H_x components

Fig (7) presents H_x measured, reconstructed by deconvolution and theoretical one.
A good agreement is shown between theoretical and reconstructed H_x component. H_x are normalized for better comparison.

5. Conclusion

Deconvolution of a probe is made by using an open waveguide and its precise model by TOM. Comparison using FEM method as COMSOL and other methods will be presented and discussed during the conference.
Probe function's application to other structures rather than open guide will be presented soon.
We mostly consider planar structures that better modelize measurement conditions of microelectronic circuits which is an interesting application for these techniques of measurements.

6. References

1. D. M. Kerns, "Plane–Wave Scattering-Matrix Theory Antennas and Antenna–Antenna Interactions", Washington U. S. Government Printing Office. NBS Monograph 162, 1981.

2. P. Silvester, "A General High-Order Finite Element Wave-guide Analysis Program," IEEE Trans. MTT, vol 4, 1969.

3. H.Baudrand, J.W.Tao & J.Atechian, "Study of radiating properties of open-ended waveguide", IEEE Trans. on Antenna & Propagation, Vol.36, pp.1071-1077, Aug.1988.

4. COMSOL Multiphysics, RF Module User's guide, COMSOL 2008.